Adaptive Grasping by Multi Fingered Hand with Tactile Sensor based on Robust Force and Position Control

Taro Takahashi, Toshimitsu Tsuboi, Takeo Kishida, Yasunori Kawanami, Satoru Shimizu, Masatsugu Iribe, Tetsuharu Fukushima, Masahiro Fujita

Intelligent System Research Laboratory, Information Technologies Laboratories, Sony Corporation
5-1-2 Kitashinagawa Shinagawa-ku, Tokyo 141-0001 Japan
[Taro.Takahashi, Toshimitsu.Tsuboi, Takeo.Kishida, Yasunori.Kawanami, Satoru.Shimizu, Masatsugu.Iribe, Tetsuharu.Fukushima, masahirof]@jp.sony.com

***Abstract*—In this paper we propose a new robust force and position control method for property-unknown objects grasping. The proposed control method is capable of selecting the force control or position control, and smooth and quick switching according to the amount of the external force. The proposed method was applied to adaptive grasping by three fingers hand which has 12 DOF, and the experimental results revealed that the smooth collision process and the stable grasping is realized even if the precise surface position, the mass and the stiffness are unknown. In addition a new algorithm determines the grasp force according to the "slip" measured with the tactile sensor and the viscoelastic media on the fingertip. This algorithm works at starting and stationary state, so the friction and mass unknown object grasping is realized by the effectual force.**

I. INTRODUCTION

With the conventional progressive researches of grasping and manipulation, we have supposed the service robot would work at home or office in the immediate future. One of the unsettled problems in this field is the property-unknown object grasping. The typical grasping strategy for property-unknown objects is (1)shape recognition by vision sensors, (2)approach with position control, (3)optimization of contact position and force and (4)grasping with force control. However, the geometrical errors result from the condition of lighting and the distance from the vision sensors. In addition, it is difficult to yield the mass, stiffness and friction of all the objects in the practical use. This paper deals with the force and position control method and adaptive grasping method.

One of the conventional approaches to force and position control is the "Hybrid Position / Force Control"[1], which is extended to the "operational space"[2]. Since the position control or the force control is selected by the "selection matrix" in these methods, it is difficult to switch each other smoothly and quickly. In the impedance control[3], the geometrical error can cause excessive force, and also the force and position control methods[1][2] have the same problem.

And some control methods of the collision process were proposed. In the method proposed in [4], using the mass-spring-damper model and linear feedback, they analyzed the stability by Lyapunov direct method. In the method proposed in [5], they use the controller including the large dumping at the collision process. However, these controllers are not designed from robustness' point of view. The force and position control based on the robust position controller[6][7] might be applied to many situations because of its robustness for the disturbance torque which becomes a problem frequently in the robot using gear drive.

In this paper we propose a new force and position control method based on the robust acceleration controller. In the proposed method, the disturbance torque (gravity, gear friction, etc.) is estimated by the disturbance observer [8] [9], whose feedback realizes the acceleration controller. And the force controller[10] is built on the acceleration controller. This controller is extended to the integrated force and position controller which has "Position Control Mode", "Force Control Mode" and "Force Constrained Position Control Mode". The third mode is capable of smooth and quick swithcing from the position controller into the force controller according to amount of the external force. This force controller starts working very well just after the collision. The proposed method was applied to a small multifingerd hand. The experimental results show the smooth collision process, robustness and quick response of force control. And stable grasping is realized even if precise surface positions, mass and stiffness are unknown.

At this experiment, the grasping posture and the grasping force are determined expediently. However, the more dexterous grasping will be realized in combination with various methods proposed in conventional researches, for example optimization of grasping force[11] and approach velocity[12]. We focus the slip sensing for dexterous grasping.

For the measurement of human-like tactile perception[13], the tactile sensors using the acceleration sensor[14], the "Acoustic Resonant Tensor Cell"[15], the strain gauge[16] and the Pressure-Conductive Rubber[17] were proposed. However, some of these experiments were not conducted with sensors mounted on the fingertip[14][15][16], and their margins for grasping force tend to be large [15][16][17].

We propose a new method of grasping force determination from the beginning to the stationary state by the slip, which is detected using the tactile sensor and the viscoelastic media on the fingertip. In the proposed method, the variable gain in force determination realizes the adaptive grasping in spite of mass and friction of the object. At stationary state, the grasping force is prevented from being too large. The effect of

Preprint submitted to 2008 IEEE International Conference on Robotics and Automation. Received September 14, 2007.

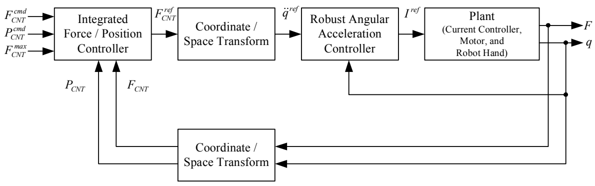

Fig. 1. The force and position controller for the adaptive grasping.

the proposed method was shown by experiments using a small multi-fingered hand.

II. Robust Force and Position Control

A. Structure of the Force and Position Robust Control

In the force and position controller for the adaptive grasping, it is desirable to design the controller so as to realize the following functions.

(a) Integrated Force and Position Control: For applications such as adaptive grasping, the position controller is useful for the approach and the force controller is useful for the grasping. In the proposed method, as in the "Hybrid Position / Force Control [1]", these controllers are selectable on each DOF (degree of freedom). In addition, one controller is able to change over another controller smoothly.

(b)External Force Limitation for Smooth Collision and Contact: The external force needs to be limited at collision and contact for stable grasping under the geometrical error. This function is realized by means of smooth and quick switching from position controller into force controller, according to the amount of the external force. In additon, it is easy to plan the grasping and the manipulation, since the external force is controlled just after the collision and the contact.

(c) Robustness of Force Control: In the assembled robot hand system, there are many factors which disturb the force control (the friction of gear, the mass of the cables, etc.). The simple modeling method of these disturbances does not make sufficient models for the computed torque method and the inverse dynamics compensation. In the proposed method, these disturbances are well compensated by the disturbance observer [8][9].

The Fig. 1 shows the force and position controller for adaptive grasping. The "plant" in Fig. 1 denotes the servo motors controlled with current controller and mechanical system. The details of each block are presented in the following section.

B. Robust Acceleration Control based on Disturbance Observer

The robust acceleration controller consists of the disturbance observer [8][9]. The total disturbance torque imposed on the system τ^{dis} is defined in (1).

$$\tau^{dis} = (J - J_n)\dot{\omega} + (K_{tn} - K_t)I^{ref} + F_c + D\omega + F^{ext} \tag{1}$$

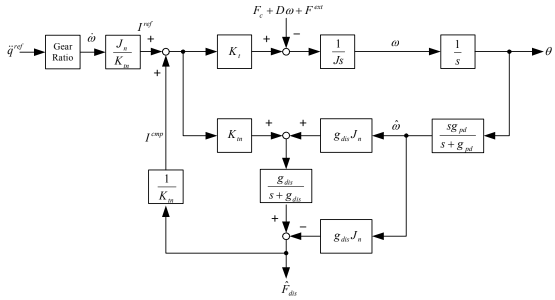

Fig. 2. Robust acceleration controller based on disturbance observer, which suppresses gravity, friction of gear and so on.

Where I^{ref} is current reference, J is inertia, K_t is torque coefficient, and ω is motor angular velocity. The lower suffix n denotes the nominal value. The first term on the right-hand side of (1) is the self-inertia variation torque, the second term models the motor torque ripples, the third term F_c is the Coulomb friction, the fourth term $D\omega$ is the viscosity friction, and the fifth term F^{ext} is the reaction force.

The total calculation process of the disturbance torque estimation is shown in (2) and Fig. 2.

$$\left.\begin{aligned} \hat{\tau}^{dis} &= \frac{g_{dis}}{s + g_{dis}}(K_{tn} I_a - sJ_n \hat{\omega}) \\ &= \frac{g_{dis}}{s + g_{dis}}(K_{tn} I_a + g_{dis} J_n \hat{\omega}) - g_{dis} J_n \hat{\omega} \\ I_a &= I^{ref} + I^{cmp} \end{aligned}\right\} \tag{2}$$

where θ is the motor angle, g_{dis} is the cutoff frequency of disturbance estimation, and g_{pd} is the cutoff frequency of pseudo-differentiator.

Since τ^{dis} is estimated through the first-order low-pass filter, it is possible to suppress τ^{dis} in the lower band than g_{dis} by the feedback of the compensation current I^{cmp} determined with $\hat{\tau}^{dis}$.

$$\hat{\tau}^{dis} = \frac{g_{dis}}{s + \frac{K_t}{K_{tn}} g_{dis}} \tau^{dis} \tag{3}$$

$$I^{cmp} = \frac{\hat{\tau}^{dis}}{K_{tn}} \tag{4}$$

When the gain J_n / K_{tn} is inserted to determine the current reference I^{ref}, Fig. 2 is the acceleration controller whose input is the acceleration reference.

Preprint submitted to 2008 IEEE International Conference on Robotics and Automation. Received September 14, 2007.

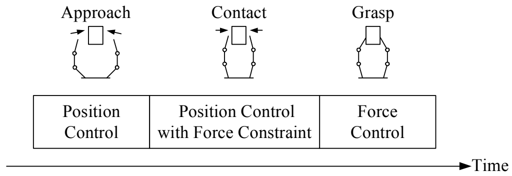

Fig. 3. Three step in the grasping motion. The external force needs to be limitead at the contact for the stable grasping under geometrical error.

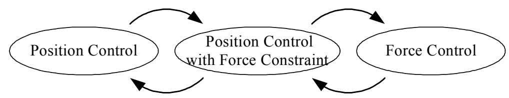

Fig. 4. The switchable three mode of controller.

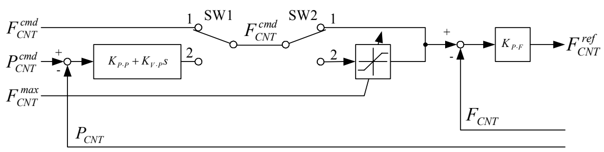

	SW1	SW2
Force Control	1	1
Position Control with force Constraint	2	2
Position Control	2	1

Fig. 5. The block diagram of force and position controller.

C. Coordinate and Space Transform

Not only the base coordinate but also the additional

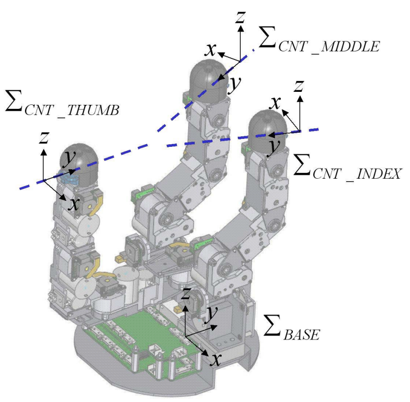

Fig. 6. The "Contact Planning Coordinate" for the grasp control.

coordinates shown in Fig. 6 are helpful to plan the grasping motion. These additional coordinates are called "Contact Planning Coordinate".

Equation (5) shows the transformation from the force reference on the contact planning coordinate F^{ref}_{CNT} into the angular acceleration reference $\ddot{q}^{ref}$.

$$\ddot{q}^{ref} = \frac{1}{J_n} Jaco^{T\,BASE}T_{CNT} F^{ref}_{CNT} \tag{5}$$

where ${}^{BASE}T_{CNT}$ denotes the translation matrix from the contact planning coordinate into the base coordinate, and the force reference at the fingertip is translated into the joint torque by transpose of the Jacobian matrix $Jaco^T$. The $\ddot{q}^{ref}$ is determined with the nominal inertia J_n.

In the conventional approach of the force control based on the robust acceleration controller [10], the $\ddot{q}^{ref}$ is calculated from the acceleration reference of the end-effector. Since this calculation needs the inverse of the Jacobian matrix $Jaco^{-1}$, the controller is not stable at the singular configuration. This problem can be avoided by the force-torque transform with $Jaco^T$ in the proposed method.

The coordinate and space transformation at the feedback is represented in (6) and (7), using direct kinematics $f(q)$.

$$F_{CNT} = {}^{CNT}T_{BASE}\,{}^{BASE}T_{ForceSensor} F \tag{6}$$

$$P_{CNT} = {}^{CNT}T_{BASE} f(q) \tag{7}$$

D. Integrated Position and Force Control

The grasp control consists of "Position Control Mode" for the approach, "Force Control Mode" for the grasping, and "Force Constrained Position Control Mode" for the collision and contact motion (Fig. 3). One control mode is able to change over another control mode, shown in Fig. 4.

In the "Force Constrained Position Control Mode", the position of the fingertip is controlled with position controller under the small external force. However, the priority of the force control is higher than the position control under the large external force in order that the external force should not go over the given "maximum external force value" F^{max}_{CNT}. In view of the grasp motion, it is desirable that the switching from the position control to the force control is smooth and quickly.

Fig. 5 shows the block diagram of this integrated force and position controller, which gives smooth and quick behavior in the "Force Constrained Position Control Mode". In addition this diagram realizes the mode change via SW1 and SW2 as described in the table. The values of the switch terminal 1 and 2 are cross-faded at SW1 for the purpose of the continuous reference. Equally, SW2 guaranties continuous transition between F^{max}_{CNT} and F^{cmd}_{CNT}, and viceversa.

At the "Force Control Mode", the force reference F^{ref}_{CNT} is calculated from the force command value F^{cmd}_{CNT} and the force sensor value F_{CNT}.

$$F^{ref}_{CNT} = K_{P\_F}\left(F^{cmd}_{CNT} - F_{CNT}\right) \tag{8}$$

TABLE I
SPECIFICATION OF THREE FINGERS HAND

Total Length / Finger Length (without wrist force sensor)	191mm / 162mm
Weight (without wrist force sensor)	1.0kg
Degree of Freedom	12
Motor Starting Torque	8.7×10^{-3} Nm, 5.6×10^{-3} Nm
Gear Ratio	1/94, 1/100, 1/118, 1/188
Back Drivablility of Planetary Gear	0.08Nm
Backlash of Planetary Gear	0.6deg
Rotary Encoder	16000pulse/rev
Force Sensor(6 axis)	3 (Fingertip) + 1 (wrist)
Tactile Sensor	3×3 mm, 38.8Hz
Maximum Force (Standard Posture)	4.0N, 2.0N
CPU	Intel Pentium4 (3.8GHz)
OS	RTLinuxPro2.2
Sampling Time of Controller	0.25msec

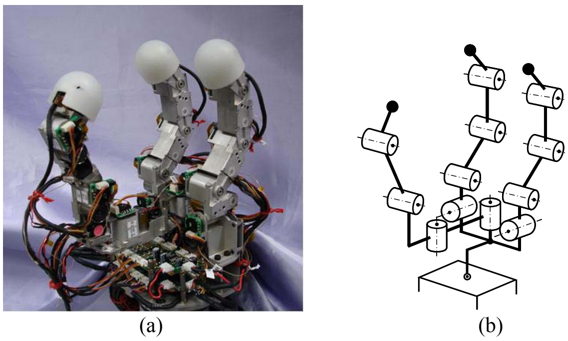

Fig. 7. Three fingers hand. (a)Appearance. (b)Configuration.

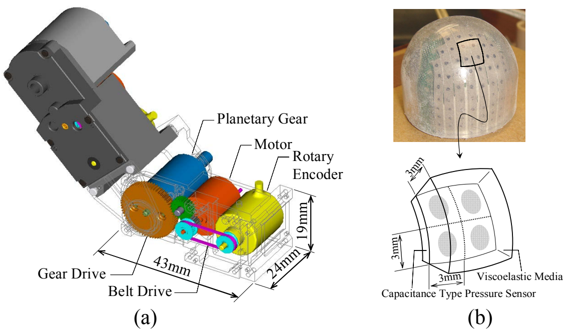

Fig. 8. (a)Joint Drive Unit (b) Tactile sensor

Fig. 9. Kamakura's Grasp Taxonomy

At the "Position Control Mode", the command value of position P_{CNT}^{cmd} generates F_{CNT}^{cmd}, and then F_{CNT}^{cmd} generates the F_{CNT}^{ref}.

$$F_{CNT}^{ref} = K_{P\_F}\left(F_{CNT}^{cmd} - F_{CNT}\right) \tag{9}$$

$$F_{CNT}^{cmd} = K_{D\_P}\left(K_{P\_P}\left(P_{CNT}^{cmd} - P_{CNT}\right) - \dot{P}_{CNT}\right) \tag{10}$$

At the "Force Constrained Position Control Mode", F_{CNT}^{cmd} is limited to F_{CNT}^{max} so that the external force might be less than F_{CNT}^{max}.

$$F_{CNT}^{ref} = \begin{cases} K_{P\_F}\left(F_{CNT}^{cmd} - F_{CNT}\right) & if \quad \left|F_{CNT}^{cmd}\right| \le F_{CNT}^{max} \\ K_{P\_F}\left(F_{CNT}^{max} - F_{CNT}\right) & if \quad F_{CNT}^{cmd} > F_{CNT}^{max} \\ K_{P\_F}\left(-F_{CNT}^{max} - F_{CNT}\right) & if \quad F_{CNT}^{cmd} < -F_{CNT}^{max} \end{cases} \tag{11}$$

$$F_{CNT}^{cmd} = K_{D\_P}\left(K_{P\_P}\left(P_{CNT}^{cmd} - P_{CNT}\right) - \dot{P}_{CNT}\right) \tag{12}$$

When the P_{CNT}^{cmd} is inside of the object surface and the finger keeps contact, $\left|F_{CNT}^{cmd}\right|$ is larger than F_{CNT}^{max}. So F_{CNT}^{ref} is equal to F_{CNT}^{max}, and the external force controlled to be equal to F_{CNT}^{max}. The characteristics of this control are the same as "Force Control Mode".

E. *Three Fingers Robot Hand*

The appearance and configuration of the three fingers hand developed for this research are shown in Fig. 7. Table I shows the specification of the hand. The total length is 191 mm, the finger length is 162 mm, and the weight is 1.0 kg. There are three fingers, and each finger has four joints. So this hand has 12 DOF, which consists of two types of small high power motor and four types of gear unit. This gear unit is composed of spur gear and planetary gear for great back drivability and strength. The planetary gear performance is shown in Table I. The small backlash especially is realized in consequence of the new planetary gear unit development.

Each joint has a 16000 pulse/rev rotary encoder, whose layout is shown in Fig. 8 (a). This parallel layout realizes the high conversion efficiency at gear unit and short length of finger.

The aims of this multi fingers hand design were maximum force, grasping posture and human-like configuration. Accordingly, the joint drive units were made up of two types of motor and four types of gear unit, considering the Kamakura's Grasp Taxonomy [18](Fig. 9). This compact multi fingered hand is capable of generating 4.0 N at the thumb fingertip and 2.0 N at the index fingertip and the middle fingertip.

The fingertip is equipped with the 6 axis force sensor and the tactile sensor, which is capable of measuring the pressure every 3 mm at 86 points for each fingertip (Fig .8 (b)). The sampling rate of the tactile sensor is 38.8 Hz. This fingertip is covered with viscoelastic media, which was designed with the finite element method (FEM) analysis (ANSYS).

This hand is mounted on the manipulator (YSKAWA Electric Corporation, MOTOMAN-UPJ), which is controlled

Preprint submitted to 2008 IEEE International Conference on Robotics and Automation. Received September 14, 2007.

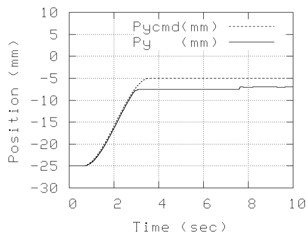

(a) Fingertip Position

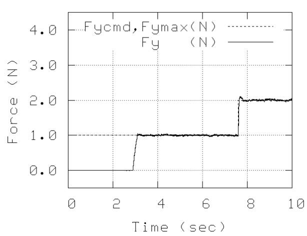

(b) Fingertip Force

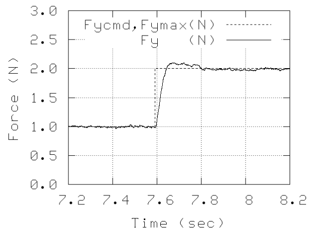

(c) Fingertip Force (Step Response)

Fig. 9. Pushing wall experiment by Proposed Method. (a)The finger started to approach at t=0.6 and went through the wall position until t=3.6. The finger collided with the wall at t=3.0, and stopped.(b) The impact force is small at the collision process (t=3.0), and the force step response (t=7.6) is excellent.(c) The time constant is 30msec.

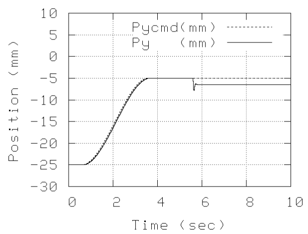

(a) Fingertip Position

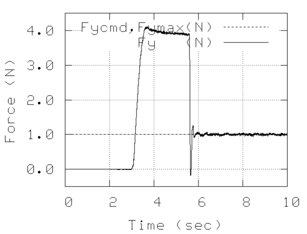

(b) Fingertip Force

Fig. 10. Pushing Wall Experiment by Conventional Approaches. (a)The finger collided with the wall at t=3.0 in position control. (b) Excessive contact force by the collision.

by the position controller with the disturbance observer and the vibration control. The controller for the hand and the manipulator is running on a PC with the RTLinuxPro 2.2, which outputs the current reference to the servo amplifier every sampling time 0.25 msec.

F. Integrated Force and Position Control Experiment

The proposed method was applied to the "Pushing Wall" experiment. The parameter in the controller g_{dis} is from 120 to 160 rad/sec, $K_{P\_P} = 50$, $K_{V\_P} = 30$ and $K_{P\_F} = 1500$. Each finger has four joints, so the controlled components are selected as $F_{CNT}^{cmd} = (f_x, f_y, m_x, m_z)$ in the thumb and $F_{CNT}^{cmd} = (f_x, f_y, f_z, m_x)$ in the index finger and middle finger. And corresponding components are selected for P_{CNT}^{cmd} .

Fig. 9 shows experimental results. At t=0, the thumb finger stopped at the side of the wall made by metal plate. The P_{CNT}^{cmd} started to approach at t=0.6 and went through the wall position until t=3.6. The finger collided with the wall at t=3.0, and stopped. The control mode is "Position Control Mode" from t=0 until t=2, "Force Constrained Position Control Mode" from t=2 until t=6, and "Force Control Mode" from t=6 until t=10. Fig. 9 (b) shows that the impact force is small at the collision process (t=3.0). Fig. 9 (c) is the enlarged graph of the force step response (t=7.6), and shows quick response whose time constant is about 30msec. This is very high performance for multi joints small robot with the gear drive. And the disturbance, for example the gear friction and the gravity for frames and cables, is suppressed well. In addition, the force and the position are smooth and continuous at the mode change (t=2 and t=6).

Fig. 10 shows results of a comparative experiment. In this experiment, the finger was controlled with position control while approaching and collision which is occurred by the the virtual geometrical error. Fig. 10 (a) dose not show the position error since position controller is working well. However the finger configuration was bended a bit. The geometrical error causes excessive contact force shown in Fig. 10 (b). The position controller was changed to force controller at t=5.5.

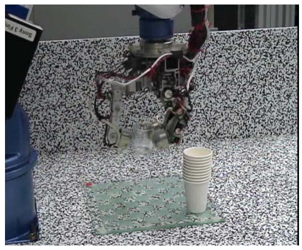
a. glass(43mm, 62g)


b. paper cup(48mm, 2.4g)


c. boiled egg(42mm, 54g, soft)

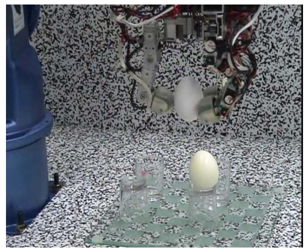
d. raw egg(43mm, 63g, hard)

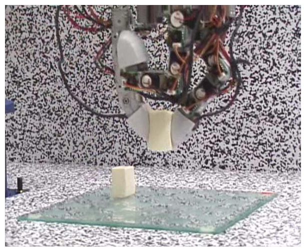
e. tofu($30\times30\times30$ mm, 36g)

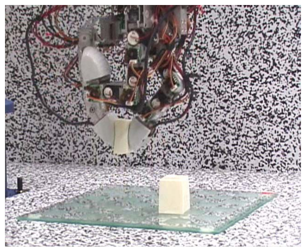
f. tofu($15\times30\times30$ mm, 20g)

Fig. 11. Grasping of objects which are various in geometry, mass, and stiffness .

III. Adaptive Grasp Control

A. Grasp Control

The proposed force and position control was applied to the "Adaptive Grasping". The "Position Control Mode" is applied for the approach and the "Force Constrained Position Control Mode" is applied for the collision and contact on the vertical axis which is illustrated with y axis in Fig. 6. For the stable grasping, the "Position Control Mode" is applied on the tangential axes which are illustrated with x and z axis. Therefore the fingertips move on the line which is parallel to vertical axis. The balanced grasping forces are decided before starting grasp in these experiments.

B. Experimental Result of Adaptive Grasping

The proposed method was applied to the grasp motion. Even if precise surface position, mass and stiffness are unknown, the proposed method makes stable grasp motion. Fig. 11 shows the grasp experiments for several kinds of objects whose size, mass and stiffness are different. While being grasped, these objects are moved by the manipulator controlled with position controller.

(a) Glass, (c) Boiled Egg without Eggshell and (d) Raw Egg are grasped with same parameter for grasp control, and contact force at thumb is 1.5 N. (b) Paper Cup is grasped with small contact force (0.25N) in order to prevent squash. Though the position of the glass was not at the set position in this experiment, the given "maximum external force" was so small (0.15N) that the finger, which collides first, kept the Glass from overturning. (e) and (f) show the grasping for various size of tofu[1] with same control parameter and same grasp force (1.0N).

IV. Adaptive Grasp Force Control Using Tactile Sensor

A. Slip extractor using tactile sensor

In the typical method, the grasping force is decided at starting grasp. In the proposed adaptive force controller, the grasping force is determined with detected slip (partial incipient slippage) in order to prevent the object from complete slipping.

The tactile sensor extracts slip by $\left(\Delta\overline{C}_{OPx}(k,i), \Delta\overline{C}_{OPy}(k,i)\right)$, which is the difference of the center of pressure (COP) for discrete-time interval i. Using a moving average of signal processing methods and the 3×3 Gaussian function of image processing functions, they reduce noise signals of tactile sensor.

Weight coefficients $K_x(i)$ and $K_y(i)$ are defined as follows. If the difference of COP $\Delta\overline{C}_{OPx}(k,i)$ is less than the threshold $i\cdot h_{Cx}$, the weight coefficient $K_x(i)$ is equal to C_s. If $\Delta\overline{C}_{OPx}(k,i)$ is greater than or equal to $i\cdot h_{Cx}$, $K_x(i)$ is equal to C_l. $K_y(i)$ is defined in a similar way.

$e_x(k,N)$ and $e_y(k,N)$ are defined as the values of the slip extractor.

[1] tofu : This Japanese tofu is the soft kind of tofu called "Silken Tofu" or "Kinugoshi Tofu (in Japanese)". This type of tofu is so soft that the "tofu steak" cannot be cooked from it.

$$e_x(k,N) = \sum_{i=1}^{2^N} K_x(i)\cdot\Delta\overline{C}_{OPx}(k,i) \qquad (13)$$

The value of the slip extractor $e_y(k,N)$ is defined in a similar way.

B. Decision of grasp force

The adaptive force controller can determine the desired grasp force based on the slip extractor values by tactile sensor using (14)

$$F^{cmd}_{CNTy}(k) = F^{cmd}_{CNTy}(k-1) + F^{slip}_{CNTy}(k) + F^{nc}_{CNTy}(k) + F^{sp}_{CNTy}(k) \qquad (14)$$

where $F^{cmd}_{CNTy}(k)$ is the desired grasp force at discrete time k, F^{slip}_{CNTy} is the term of the increases in the desired grasp force calculated by the value of the slip extractor, F^{nc}_{CNTy} is the term of the cancellation of the much increases caused by the noise signals of the slip extractor, F^{sp}_{CNTy} is the term of the suppression of the desired grasp force.

In order to prevent the object from slipping in any direction, the value of the slip extractor to all directions is defined

$$e_{Sx}(k) = \left|\sum_{j=1}^{3} e_x(k,j)\right| \qquad (15)$$

$e_{Sy}(k)$ is defined in a similar way.

The value of increases in the desired grasp force is defined as (16)

$$F^{slipx}_{CNTy}(k) = \sum_{i=0}^{N_f-1} f_i(k)\cdot G_{Sxi}(e_{Sxi}(k))\cdot e_{Sxi}(k) \qquad (16)$$

$$G_{Sxi}(e_{Sxi}(k)) = \frac{m_i}{T_c}\cdot\left\{C_{Sc} + \frac{G_S}{1+\exp(-e_{Sxi}(k)+O_S)}\right\} \qquad (17)$$

where $F^{slip}_{CNTy} = F^{slipx}_{CNTy} + F^{slipy}_{CNTy}$ is the value of increases in the desired grasp force, F^{slipx}_{CNTy} and F^{slipy}_{CNTy} are the values based on the value of the slip extractor component of x and y, N_f is the index number of the three fingers, m_i is the weight value of each finger, f_i is the normal force sensing by pressure sensor, T_C is the adjustment value of difference between the control cycle and the measurement cycle, G_{Sx} is the variable gain, C_{Sc} is the constant value, G_S is the coefficient of the sigmoid function, O_S is the offset of the sigmoid function. F^{slipy}_{CNTy} and G_{Syi} are defined in a similar way.

F^{nc}_{CNTy} and F^{sp}_{CNTy} are calculated if F^{slip}_{CNTy} is less than h_{slip}. The values of the cancellation of the increases of the grasp force due to noise signals are balanced by the term defined in (18)

$$F_{CNTy}^{ncx}(k) = \sum_{i=0}^{N_f-1} f_i(k) \cdot G_{Snxi}(e_{Sxi}(k)) \cdot \{e_{Sxi}(k) - C_{sn}\} \tag{18}$$

$$G_{Snxi}(e_{Sxi}(k)) = \frac{m_i}{T_c} \cdot \left\{ \frac{G_{sn}}{1+\exp\left(a_{sn} \cdot (e_{Sxi}(k) - O_{sn})\right)} \right\} \tag{19}$$

where $F_{CNTy}^{nc} = F_{CNTy}^{ncx} + F_{CNTy}^{ncy}$ is the value of the cancellation of the increases of the grasp force due to noise signals, F_{CNTy}^{ncx} and F_{CNTy}^{ncy} are the value based on the value of the slip extractor component of x and y, G_{Snx} is the variable gain, G_{Sn} is the coefficient of the sigmoid function, O_{Sn} is the offset of the sigmoid function, a_{Sn} is the coefficient of exponential function of the sigmoid function. F_{CNTy}^{ncy} and G_{Snyi} are defined in a similar way.

The value of the suppression of the desired grasp force is defined in (20)

$$F_{CNTy}^{sp}(k) = \begin{cases} \sum_{i=0}^{N_f-1} f_i(k) \cdot \frac{m_i}{T_c} \cdot \left[G_{px} \cdot \{\bar{e}_{Sxi}(k) - h_{pxi}\} + G_{py} \cdot \{\bar{e}_{Syi}(k) - h_{pyi}\} \right] & \left(if \quad \bar{e}_{Sx} < h_{px} \cap \bar{e}_{Sy} < h_{py}\right) \\ 0 & \left(if \quad \bar{e}_{Sx} \geq h_{px} \cup \bar{e}_{Sy} \geq h_{py}\right) \end{cases} \tag{20}$$

where F_{CNTy}^{sp} is the value of the suppression of the desired grasp force, G_{px} and G_{py} are the gains, $\bar{e}_{Sx}(k)$ and $\bar{e}_{Sy}(k)$ are the values of the moving average of $e_{Sx}(k)$ and $e_{Sy}(k)$, h_{px} and h_{py} are the constant values, α is a constant value greater than 1.

C. Experimental setup and results

In this experiment, a cylinder wrapped copier paper (52g) and additional weights (0g, 100g, 200g and 300g) are grasped. The grasping force of each finger satisfies equilibrium of force. The three fingers initially contact to the object with a thumb grasp force of 0.3N. At t=0.6s the manipulator begins lifting up. At 5.6-16s the object is kept at the height of 40mm. The desired grasp force F_{CNTy}^{cmd} must be less than or equal to initial grasp force. Table II shows all the values of the parameters.

We also introduce the experiment is performed in an early stage of research. The manipulated object is a cube with powder. The object is very slippery. The three fingers initially contact the object with a thumb grasp force of 1.0N. At t=0.6s the manipulator tries to lift at the height of 40mm in 5s. F_{CNTy}^{cmd} is defined in (21).

TABLE II
PARAMETERS OF GRASP FORCE CONTROLER

parameter	value	parameter	value
h_{Cx}, h_{Cy}	0.1 (if N=1)	C_S	1.0
h_{Cx}, h_{Cy}	0.01 (if N=2)	Cl	2.0
h_{Cx}, h_{Cy}	0.005 (if N=3)		
N_f	3	C_{sn}	0.04
T_c	500	G_{sn}	0.015
m_0	2.5	O_{sn}	0.012
m_1, m_2	1.25	a_{sn}	1000
C_{sc}	0.002	h_{px0}, h_{py0}	0.075
G_s	0.013	h_{px1}, h_{py1}	0.025
O_s	2.0	h_{px2}, h_{py2}	0.005
h_{slip}	0.005	G_{px}	0.15
α	1.5	G_{py}	0

$$F_{CNTy}^{cmd}(k) = F_{CNTy}^{cmd}(k-1) + F_{CNTy}^{slip}(k) - \sum_{i=0}^{N_f-1} G_O \cdot f_i(k) \tag{21}$$

$$G_O = C_O \cdot m_i / T_C \tag{22}$$

where G_O is the constant gain, C_O is the constant value. The constant force experiment is performed as comparison experiment. The parameters are $C_{Sc} = 0.20$, $G_S = 0$, $C_O = 0.017$ for constant gain.

Figure 12 shows sample test data with 200g weight. It shows detailed plots of grasp force F_{y0} observed by 6 axis force sensor, desired value F_{CNTy}^{cmd} , normal force f_0 by slip sensor, $e_{Sx}(k)$, $\bar{e}_{Sx}(k)$, $e_{Sy}(k)$, and $\bar{e}_{Sy}(k)$.

Figure 13 shows plots of desired value $F_{CNTy}^{cmd}(k)$ with 100, 200, 300g weight and no weight. As shown in Figure 13, at time 2-4 seconds, the desired force values reach the maximum value by F_{CNTy}^{slip} , and reach the steady value at 3-10 seconds afterwards by F_{CNTy}^{nc} and F_{CNTy}^{sp} . The larger the mass, the faster they reach the maximum value.

Figure 14 shows plots of relation between the desired grasp force and the mass. The maximum value and the steady value of the desired force increase in proportion to the mass of the object. We have found that sensing the difference of the center of pressure is an effective method to decide the grasp force.

Figure 15 shows desired value $F_{CNTy}^{cmd}(k)$ for slippery cube grasping. By the proposed method, the adaptive grasping force reaches 2.8N and attains the grasping. However, the constant force without the proposed method can not attain the grasping.

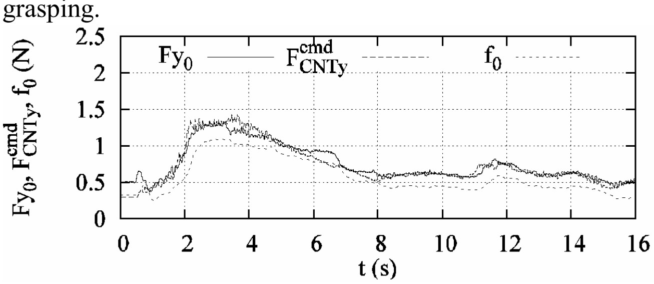

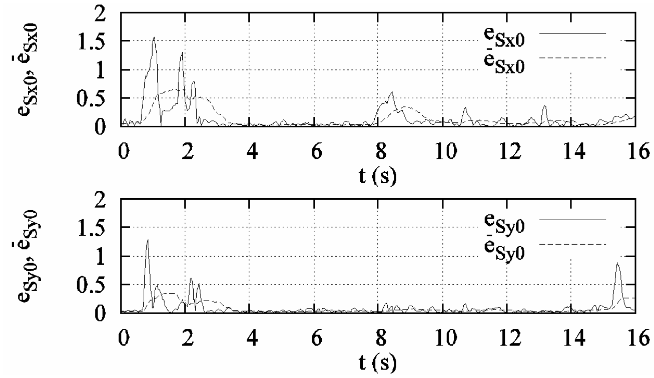

Fig. 12: Experimental result 200(g)

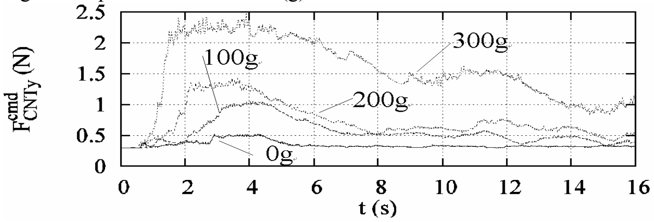

Fig. 13: Experimental result 10-300(g)

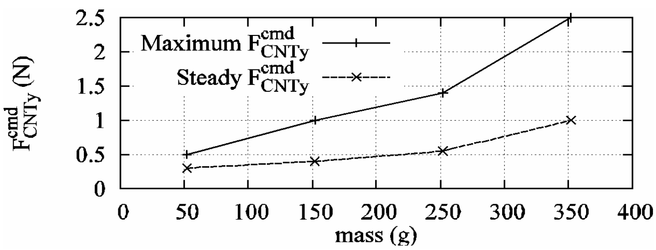

Fig. 14: Experimental result 0-300(g)

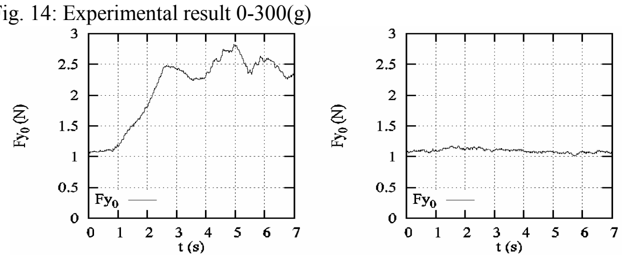
Fig.15: Experimental result (grasping the slippery cube)

V. CONCLUSION

In this paper we proposed the novel force and position controller for property-unknown objects grasping. The proposed method is capable of smooth and quick swithcing from position controller into force controller according to the amount of the external force. The experimental resutls on the small 12 DOF multi fingered hand showed that collision process was smooth and force control respons was quick (time constant is 30msec.). The proposed method realized the stable grasping for glasses, paper cups, eggs and tofu whose precise surface position, mass and stiffness were unknown. In addition a new algorithm was proposed, which determined the effectual grasping force with the tactile sensor. In the proposed method, the grasping force proportionate to mass is determined without mass-sensing, and the friction unknown object grasping was realized. The effect of the proposed method was shown by experiments using the small three fingers hand.

ACKNOWLEDGMENT

The authors would like to thank Dr. A. Iga, the head manager of the Information Technologies Laboratories, and all the persons concerned in this research.

REFERENCES

[1] M.H.Raibert , John J.Craig: “Hybrid Position/ Force Control of Manipulators,” Journal of Dynamic Systems, Measurement, and Control 102, ASME, pp.126-133,1981

[2] O. Khatib: A Unified Approach for Motion and Force Control of Robot Manipulators: The Operational Space Formulation, IEEE Journal of Robotics and Automation, Vol.RA-3, No.1, 1987

[3] N. Hogan: Impeedance Control: An Approach to Manipulation: Part 1-3, Journal of Dynamic Systems, Measurement, and Control 107, ASME, 1985

[4] Y. Shoji, M. Inaba, T. Fukuda: “Impact Control of Grasping,” IEEE Transactions on Industrial Electronics, Vol. 38, No. 3, pp. 187-194, 1991

[5] O. Khatib, J.Burdic: Motion and Force Control of Robot Manipulators, IEEE Conference on Robotics and Automation,pp.1381-1386,1986

[6] Y.Hori, K.Shimura and M.Tomizuka, Position/Force Control of Multi-Axis Robot Manipulator based on the TDOF Robust Servo Controller for Each Joint, 11th American Control Conference, 1992

[7] K.Shimura and Y.Hori, Position, Collision and Force Controls of Robot Manipulator based on the Robustified Joint Servosystem, 2nd AMC Conference, 16-25, 1992

[8] K. Ohishi, K. Ohnishi, K. Miyachi: “Torque-Speed Regulation of DC Motor Based on Load Torque Estimation,” Proceedings of the IEEJ International Power Electronics Conference, IPEC-TOKYO, Vol. 2, pp. 1209-1216, 1983

[9] K. Ohnishi, M. Shibata, T. Murakami: “Motion Control for Advanced Mechatronics,” IEEE/ASME Transactions on Mechatronics, Vol. 1, No. 1, pp. 56-67, 1996

[10] T. Murakami, T. Yu, F. Ohnishi, K., “Torque sensorless control in multidegree-of-freedom manipulator,” IEEE Transactions on Industrial Electronics, Vol. 40, No. 2, pp. 259-265, 1993

[11] Jeffrey Kerr, Bernard Roth: “Analysis of Multifingered Hands,” International Journal of Robotics Research, Vol. 4, No. 4, pp. 3-17, 1986

[12] K. Kitagaki, M. Uchiyama: “Optimal approach velocity of end-effector to the environment,” IEEE International Conference on Robotics and Automation, vol.3, pp.1928 - 1934, 1992

[13] R. S. Johansson and G. Westling "Roles of glabrous skin receptors and sensorimotor memory in automatic control of precision grip when lifting rougher or more slippery objects," Experimental Brain Research 56, 1984, pp. 550-564.[1]

[14] M. R. Tremblay and M. R. Cutkosky "Estimating Friction Using Incipient Slip Sensing During a Manipulation Task," IEEE International conference on robotics and automation, 1993, pp.429-434[4]

[15] T. Yoshikai, R. Tajima, S. Kagami, H. Shinoda, M. Inaba and H. Inoue "Slip detecting by tactile sensor using Acoustic Resonant Tensor Cell and its application for grasping," JRSJ vol. 20, No.8, 2002, pp.868-875 (in Japanese)

[16] T. Maeno, S. Hiromitsu and T. Kawai: “Control of grasping force by detecting stick/slip distribution at the curved surface of an elastic finger,” IEEE Conference on Robotics and Automation, pp. 3895-3900, 2000

[17] D. Gunj Y. Mizoguchi, A. Ming, A. Namiki, M. Ishikawa and Shimojo "Grasping Force Control of Multi-fingered Robot Hand based on Slip Detection," Proceedings of the 2007 JSME Conference on Robotics and Mechatoronics, May, 2007, 1A2-B07 (in Japanese)

[18] N.Kamakura, M.Matsuo, H.Ishii, F.Mitsubosi and Y.Miura, “Patterns of static prehension innormal hands,” American Journal of Occupational Therapy, 34, 7, pp. 437-445, 1980